Polymer 50 (2009) 5406–5413

Contents lists available at ScienceDirect

Polymer

journal homepage: www.elsevier.com/locate/polymer

Effect of water concentration on photopolymerized acrylate/epoxide hybrid polymer coatings as demonstrated by Raman spectroscopy

Ying Cai, Julie L.P. Jessop*

Department of Chemical and Biochemical Engineering, University of Iowa, 4133 Seamans Center, Iowa City, IA 52242, USA

ARTICLE INFO

Article history:
Received 30 October 2008
Received in revised form
4 September 2009
Accepted 12 September 2009
Available online 18 September 2009

Keywords:
Photopolymerized epoxide/
acrylate hybrid coatings
Raman confocal microscopy
Depth-profiling

ABSTRACT

Photopolymerization systems based on hybrid monomer 3,4-epoxy-cyclohexylmethyl methacrylate (METHB) were studied to investigate water effects on conversion and polymer coating properties. METHB contains epoxide and methacrylate moieties, which undergo cationic and free-radical photopolymerization, respectively. The conversion of both groups was obtained by Raman spectroscopy in real time and depth. Water concentration and initiator system compositions were varied and shown to affect reaction kinetics and depth profile. With increasing water concentration, the epoxide induction period increased when only cationic initiator was present; however, the induction period disappeared when using the dual-initiator system. In addition, epoxide groups continued reacting after light was shuttered and reached a higher and more homogeneous conversion. Hybrid systems were shown to be less sensitive to water at low or intermediate concentrations. With high water concentrations, hybrid monomer systems manifested increased ring opening during illumination due to chain transfer and decreased physical properties due to loss of cross-linking.

1. Introduction

Photopolymerization has been widely used in coatings, inks, adhesives, and dental composites because of its efficiency, economic and energy savings, and environmentally friendliness [1–3]. With the advent of effective photoinitiators, such as diaryliodonium and triarylsulfonium salts [1,4,5], cationic photopolymerization, with its advantages of oxygen insensitivity, low toxicity, and shrinkage, has become a possible alternative to traditional free-radical photopolymerization systems [6]. In recent years, cationic and free-radical systems have been combined to form hybrid photopolymerization systems. Monomer mixture hybrid systems, such as acrylate/epoxide [7–11] and epoxy/vinyl ether [9,12–14], incorporate two monomers bearing different functional groups, which undergo free-radical and cationic polymerization separately. Monomers with both epoxide and vinyl ether [15] or epoxide and acrylate [16] moieties have also been synthesized and investigated. Although free-radical and cationic ring-opening photopolymerization systems are sensitive to oxygen and humidity, respectively, the hybrid coatings polymerized by dual cationic/free-radical photoinitiator systems have shown less sensitivity to both atmospheric factors. These so-called hybrid photopolymerizations combine the advantages of the two reaction pathways and offer new and improved coating formulation strategies. However, the interactions between the two reaction pathways and the impact of environmental inhibitors upon the hybrid systems have yet to be understood fully. A better understanding of these hybrid systems would enable their purposeful formulation for widespread use throughout the photopolymerization industry. Successful introduction of hybrid systems could decrease costs associated with combating oxygen inhibition, facilitate faster reactions, decrease the dependence of product quality upon humidity conditions in the manufacturing environment, provide polymers with better surface properties, and permit the production of thin films at ambient conditions. Previous work probed the effects of oxygen in an acrylate/epoxide hybrid monomer system [16]; this paper focuses on the effects of water in the system.

Water and other proton donors serve multiple roles in cationic polymerizations and can significantly impact the resulting polymer properties [1,17–20]. Extensive research [17,19,21–24] has been conducted to elucidate the mechanisms of reactions involving proton donors during cationic polymerizations. First, proton donors are required in the decomposition of the onium salt cationic photoinitiator. Generation of initiating super acids (initiation step in Scheme 1) leads to the formation of cationic active centers. However, an excessive amount of water can deactivate the initiator and inhibit the reaction through hydrolysis of the organic cation and anion of the super acid [25]. The cationic active centers can start a propagating chain as described in Scheme 1 through an active chain end (ACE)

* Corresponding author. Tel.: +1 319 335 0681; fax: +1 319 335 1415.
E-mail address: jjessop@engineering.uiowa.edu (J.L.P. Jessop).

0032-3861/$ – see front matter © 2009 Elsevier Ltd. All rights reserved.
doi:10.1016/j.polymer.2009.09.031

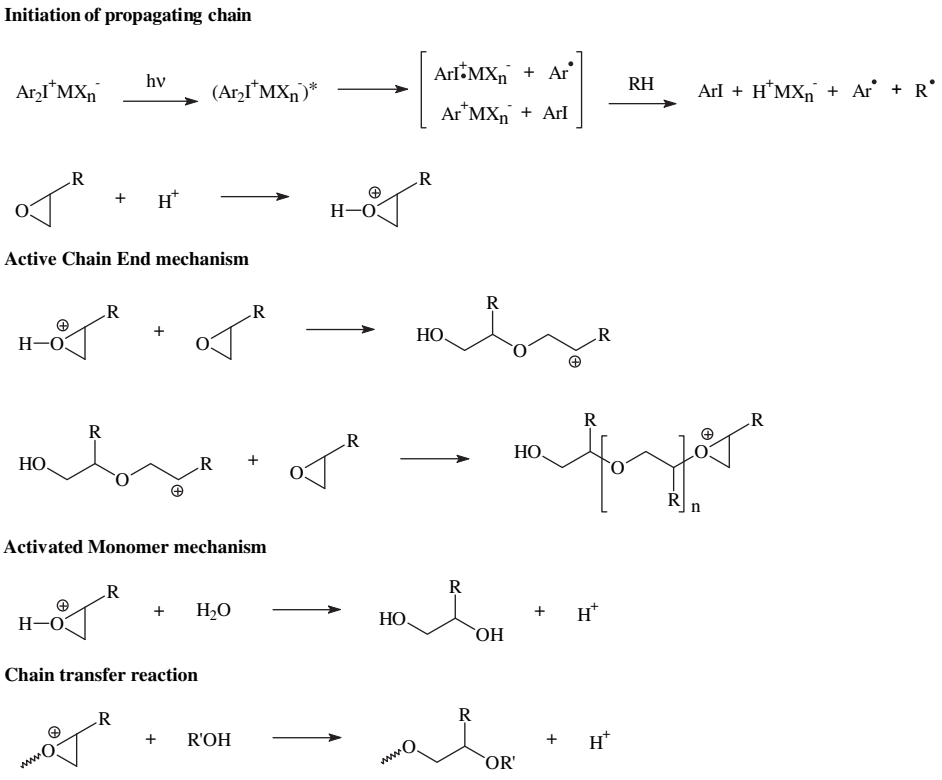

Scheme 1.

mechanism or react with hydrogen donors like water through an activated monomer (AM) mechanism [22,24,26]. Reactivity of cationic active centers with monomer or water determines the balance between the two mechanisms. In addition, the structural effect of the monomers has been reported. For example, cations formed in a system of vinyl ether without –OH end groups has been shown to react faster with water than with another monomer [27]. Although water can react as a termination agent and inhibit the chain propagation, the activated monomers (e.g., diols formed through the AM mechanism) can start chain transfer reaction with cationic centers as shown in Scheme 1. This mechanism competes with the ACE mechanism and may contribute significantly to monomer depletion and affect the chemical structure and physical properties of the resulting polymer due to formation of shorter polymer chains or polymer networks with lower cross-linking density. In hybrid systems comprising both free-radical and cationic reactions, the impact of water is even more complicated and convoluted because the initiation and propagation of one reaction affects the other.

In this study, hybrid photopolymerizations were monitored by real-time Raman spectroscopy, and profiles of functional group conversions at various depths in the cured coating samples were investigated by Raman confocal microscopy. Real-time Raman spectroscopy has been an effective reaction monitoring tool because of the advantages of high time resolution, detection of multiple functional groups, and minimum sample handling [28]. The combination of confocal microscopy and Raman spectroscopy also provides an unique technique to investigate conversion depth profiles in multilayer polymer coatings and films of several tens of microns without actually touching the sample [16,29,30]. This technique has been used in a prior study [16] to determine the effect of oxygen inhibition upon these hybrid coatings, as well as by other researchers to determine chemical compositions [29,31,32].

The kinetic mechanisms of the two parallel reactions in this acrylate/epoxide hybrid system revealed how water, as a complicated player in cationic photopolymerization, impacted the epoxide ring-opening reaction. In addition, the synergistic effects of the photo-initiators were highlighted in the dual-initiated hybrid system. The spatial characteristics of the polymer network, as well as the benefits of epoxide dark polymerization, were demonstrated through conversion depth profiles of the acrylate and epoxide functional groups. Finally, the physical properties of the resulting hybrid coatings were evaluated and correlated with the depth profiles and kinetic results to link the fundamental research directly with applications in coatings and films.

2. Experimental

2.1. Materials

3,4-Epoxy-cyclohexyl-methyl methacrylate (METHB, Diacel) (see Fig. 1) was the methacrylate/epoxide hybrid monomer used in this study. The water concentration of the monomer was 758 ppm, as determined by Karl–Fischer titration (Aquastar® C2000 Coulometric Titrator, EM Science). Additional distilled, deionized water was added into each formulation to obtain the desired water concentration. The α-cleavable free-radical initiator 2,2-dimethoxy-2-phenyl-acetophenone (DMPA, Aldrich) was used to initiate the reaction of the (meth)acrylate C=C double bond, and the cationic photoinitiator diaryliodonium hexafluoroantimonate (DAI, Sartomer) was used to

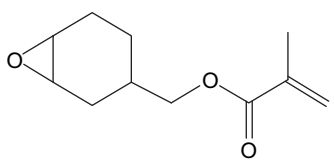

Fig. 1. Molecular structure of hybrid monomer METHB.

induce the photopolymerization of the cycloaliphatic epoxide ring. All materials were used as received. For single-initiator systems, 0.5 wt% DMPA or DAI was used, and a combination of 0.5 wt% DMPA and 0.5 wt% DAI was used as a dual-initiator system.

2.2. Methods

2.2.1. Raman spectroscopy

Real-time Raman spectra were collected using a holographic fiber-coupled stretch probehead (Mark II, Kaiser Optical Systems, Inc.) attached to a modular research Raman spectrograph (HoloLab 5000R, Kaiser Optical Systems, Inc.). A 10× non-contact sampling objective with 0.8-cm working distance was used to deliver ~200 mW 785 nm near-infrared laser intensity to the sample, thereby inducing the Raman scattering effect. The exposure time for each spectrum was 500 ms, and the time interval between data points was ~700 ms. Samples were photopolymerized at room temperature in sealed 1 mm ID quartz capillary tubes using a 100 W high-pressure mercury lamp (Acticure® Ultraviolet/Visible Spot Cure System, EXFO Photonic Solutions, Inc.). The output lines from this lamp in the ultraviolet spectral region are at 254, 297–302, 312–313, 334, and 365 nm, which coincide with the absorption of DMPA (225–380 nm with $\lambda_{max} = 250$ and 340 nm in methanol) [33] and DAI (190–340 nm with $\lambda_{max} = 220$ and 245 nm in methanol). The full-spectrum light intensity of the system was set to 100 mW/cm^2. Each real-time experiment was repeated 3–5 times, and the standard deviation in the resulting acrylate and epoxide conversion profiles was ±0.02–0.04.

An optical microscope (DMLP, Leica Microsystems GmbH) with confocal optics attached to the modular research Raman spectrograph was used to obtain spectra of monomer and depth profiles of photopolymer coatings. A combination of 785 nm single-mode excitation fiber and 15 μm collection fiber was used for all microscopic studies. A 10× objective with numerical aperture equal to 0.25 and with 5.8 mm working distance was used to study the monomer. The laser beam delivered from the 10× objective to the sample was ~9 mW in intensity for microscopic studies. The exposure time for monomer spectra was 5 s. For depth-profiling studies, the monomer mixture was spread on a quartz slide using a razor blade and photopolymerized for 45 min to reach the highest conversion with the 100 W high-pressure mercury lamp at a light intensity of 100 mW/cm^2 under ambient conditions (20 °C and 40 ± 5% relative humidity). The thickness of the finished coatings was about 100 μm. An 100× objective with numerical aperture equal to 0.9 and with 0.27 mm working distance was used to study the coatings. This confocal setup provided a spot size of 1.5 μm and depth resolution of 3 μm. The exposure time for depth-profiling studies was set to 120 s to optimize the signal-to-noise ratio. Raman spectra of the coatings were taken starting from the sample surface to ~60 μm within the sample using 4 or 5 μm step sizes to ensure isolated sampling volumes. Depth profiling of the coatings was performed immediately after photopolymerization and after 24 h on the microscope stage in the dark to determine if any dark polymerization occurred. The stability of the confocal microscope was tested by collecting 5 spectra at various locations within a specimen, and the standard deviation in the resulting acrylate and epoxide conversions was ±0.04.

The Raman spectrum of METHB was acquired first to identify bands in the fingerprint region that could be used to calculate conversion (see Fig. 2). The reactive band representing the methacrylate C=C double bond is located at 1640 cm^{-1} and is associated with the C=C stretching vibrations [34,35]; the reactive band representing the epoxide ring is located at 790 cm^{-1} and is associated with the symmetric epoxide ring deformation [22,36]. An internal reference band was selected at 605 cm^{-1}, which represents the stretching of the non-reactive methacrylate carbonyl (C–C–O) group [34,35]. The peak areas under each band were integrated and

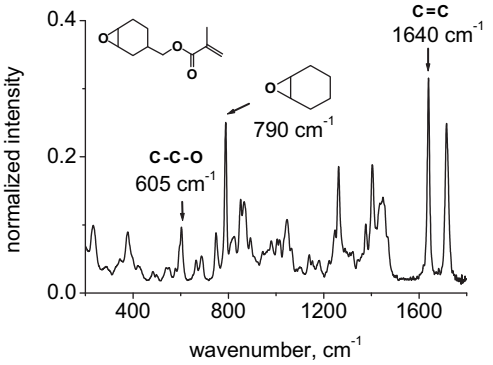

Fig. 2. Characteristic peaks in Raman spectrum of hybrid monomer METHB: CCO internal reference band at 605 cm^{-1}, epoxide ring reactive band at 790 cm^{-1}, and C=C double bond reactive band at 1640 cm^{-1}.

used to calculate the concentration of related functional groups. Since the spectral baselines and the reference band intensity remained constant in the real-time studies, the conversion of each functional group was calculated by ratioing the concentration of the functional group at any given time [$A_{rxn}(t)$] to the initial concentration [$A_{rxn}(0)$]:

$$\text{conversion}, \alpha = 1 - A_{rxn}(t)/A_{rxn}(0) \quad (1)$$

These results were compared with conversions calculated using peak areas resolved after taking the second derivative of each spectrum using first the chosen characteristic peaks (i.e., 1640 and 790 cm^{-1}) and then other peaks associated with same functional groups (e.g., 1410 cm^{-1} for the C=C). The differences between these methods were within the experimental error for this specific monomer, so the results are all reported using Equation (1). In the depth-profiling studies, the peak area of the internal reference band [A_{ref}] was used to eliminate the effect of the decreasing signal-to-noise ratio as the sampling depth increased and to enable comparison of measurements at different times:

$$\text{conversion}, \alpha = 1 - \frac{A_{rxn}(t)/A_{ref}(t)}{A_{rxn}(0)/A_{ref}(0)} \quad (2)$$

2.2.2. Physical property testing

Photopolymerized coatings were then tested to obtain surface hardness, glass transition temperature (T_g), and storage modulus. For this physical property testing, the monomer mixture was spread on a quartz slide using drawdown blocks and photopolymerized for 45 min with the 100 W high-pressure mercury lamp at a light intensity of 100 mW/cm^2 under ambient conditions. The thickness of the finished coatings was about 250 μm. The surface quality was determined by the film hardness by the pencil test based on ASTM D3363-00. The coatings were removed by razor blade from the substrate to obtain free films, 3–5 mm wide by 6–8 mm long, which were tested by a dynamic mechanical analyzer (Q800, TA Instruments) using a film tension clamp. A temperature ramp from −80 °C to 250 °C at a frequency of 1 Hz and 3 °C/min ramping rate was performed on the films with three replicates for each formulation. The T_g of the films was determined by the tan δ peak.

3. Results and discussion

These studies investigated the effect of water concentration on photopolymerizations of the methacrylate/epoxide hybrid monomer METHB with three different initiation systems: free-radical initiator only, cationic initiator only, and dual-initiator system. The

reactions were studied by real-time Raman spectroscopy, and the coatings cured in ambient conditions were depth-profiled using Raman confocal microscopy and tested to obtain physical properties. The connections among fundamental reaction kinetics, the resulting chemical structure, and the final product properties provide guidance for improving and tailoring the performance of these hybrid photopolymer coatings.

3.1. Free-radical initiator only system

The effect of water concentration upon coatings with METHB and only the free-radical initiator DMPA was studied using real-time Raman spectroscopy. Increasing water concentration slowed down the reaction rate of the C=C double bond, but did not affect the induction period, time to ultimate conversion, or ultimate conversion (see Fig. 3). During the bulk of the photopolymerization (*i.e.*, 50–400 s timeframe), the reaction rate for systems with no water added was approximately 4% higher than that of systems with 1.5 wt% water added. Here, water acted as a plasticizer, enhancing the mobility of the reactive species and delaying the onset of autoacceleration [20].

3.2. Cationic initiator only system

The effect of water concentration upon coatings with METHB and only the cationic initiator DAI was studied using Raman spectroscopy and microscopy. Although radicals are generated during the production of the cationic active centers (Scheme 1), they are not able to initiate the free-radical polymerization of the methacrylate at low temperatures [16]; thus, only the cationic ring-opening polymerization is discussed here. In cationic ring-opening polymerizations, water serves multiple functions: a hydrogen donor, an inhibitor, and a chain-transfer agent. Fig. 4 shows, in real time, the effect of increasing water concentration on the epoxide ring-opening reaction of METHB initiated only by 0.5 wt% DAI. An extended induction period was observed with increasing water concentration because high concentrations of water can inhibit cationic polymerization of the epoxide ring by deactivating the initiator through hydrolysis [25]. After the initial induction period, the reaction rate of the formulation with 1.5 wt% water tripled compared to the formulation with no water added. After 700 s of illumination, the conversion of the formulation with 1.5 wt% water was over 30%, whereas the conversion of the formulation with no water added was 20%. Similar phenomena of increased reaction rate and conversion were reported to occur for a cycloaliphatic epoxide cationic photopolymerization system via extensive chain transfer reaction due to the addition of

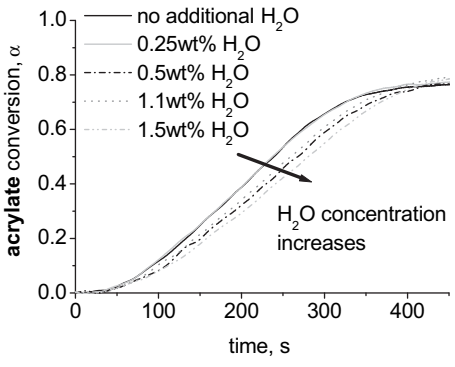

Fig. 3. Conversion profiles (by real-time Raman spectroscopy) of METHB formulated with different water concentrations and photopolymerized with 0.5 wt% free-radical initiator DMPA only. Samples were cured with 100 mW/cm^2 initiation light intensity at room temperature.

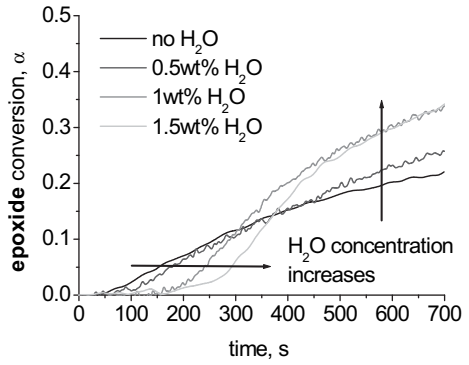

Fig. 4. Conversion profiles (by real-time Raman spectroscopy) of METHB formulated with different water concentrations and photopolymerized with 0.5 wt% cationic initiator DAI only. Samples were cured with 100 mW/cm^2 initiation light intensity at room temperature.

hydroxyl-containing compounds, such as water and alcohols [17,25]. After cationic centers are generated, they can react with water through the ACE mechanism or with unreacted epoxide rings though the AM mechanism. ACE and AM mechanisms compete with one other as the reactions progress, and their balance determines which mechanism supersedes the other. Compared to cycloaliphatic epoxide rings, the water or alcohol molecules are smaller in size, making it easier for them to attack the chain-end cations, which are shielded by hexafluoroantimonate anions that hinder access by the next monomer [18]. Thus, for METHB, the monomers may have reacted rapidly with water first to form alcohols through the AM mechanism. Then, these alcohols could act as efficient chain transfer agents to boost the reaction rate and conversion.

The coatings cured in ambient conditions were then examined by Raman confocal microscopy immediately after 45-min illumination (*i.e.*, 0-h dark polymerization in Fig. 5), and these depth profiles of three coatings with different water concentrations are shown as solid lines in Fig. 5. As with the real-time experimental results, the average epoxide ring conversions immediately after 45-min illumination were higher when water was added to the formulation. More homogeneous epoxide conversions were observed for coatings with water added, while decreased epoxide ring conversion with increasing depth was observed for coatings without water added. Light penetration to the bottom of the sample is hindered by the absorption characteristics of the upper layers, resulting in decreased active center concentration and ultimately low conversion at greater sample depths. However, the effect of light penetration would be less

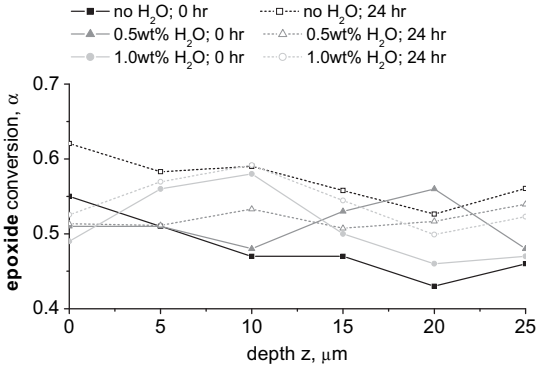

Fig. 5. Depth profiles (by Raman confocal microscopy) of epoxide ring conversion in METHB formulated with different water concentrations and photopolymerized with 0.5 wt% cationic initiator DAI only. Solid lines and dotted lines were taken at 0 and 24 h after illumination, respectively. Samples were cured with 100 mW/cm^2 initiation light intensity at ambient conditions.

profound for coatings with water added since the epoxide rings can undergo the AM mechanism, as well as the ACE mechanism. The extensive chain transfer reaction and effective reaction diffusion would facilitate active center migration to greater sample depths, thereby increasing the conversion of epoxide rings in the coating interior.

After the samples were stored in the dark for 24 h, the coatings were depth-profiled again to study the dark polymerization, and the results are shown as dotted lines in Fig. 5. Dark polymerization occurred due to the long-lived nature of cationic active centers as evidenced by higher and more homogeneous epoxide ring conversion throughout the coating than measured immediately after 45-min illumination. However, in contrast with the 0-h results, the coating without water added showed the highest average epoxide ring conversion, and the increase in the overall conversion was higher than in the coatings with water added. For the METHB coating without water added, more active centers could be generated in the absence of water inhibiting the initiation through the deactivation of DAI.

3.3. Dual-initiator system

Finally, the effect of water concentration upon coatings with METHB and both the free-radical initiator DMPA and the cationic initiator DAI were studied using Raman spectroscopy (see Fig. 6). The reaction rate of the C═C double bond decreased, and the final conversion increased with increasing water concentration due to the plasticizing effect of the water. After the same illumination time, the conversion of the epoxide ring drastically increased as the water concentration increased due to extensive chain transfer reaction: the epoxide ring conversion of the formulation with 1.5 wt% water tripled compared to the formulation with no water added. However, there was no dependence of the cationic induction period on the water concentration. This may be caused by lower sensitivity to moisture in the dual-initiator system, in which decomposition of the cationic initiator is promoted by free-radicals [37–39]. In this so-called free-radical promoted cationic polymerization mechanism, DAI decomposition results, not through the absorption of light, but through a re-dox reaction with free radicals, which are generated through the photodecomposition of DMPA. This decomposition pathway was confirmed by in-house experiments of a bifunctional cycloaliphatic epoxide monomer with the same dual-photoinitiator system. In this experiment, epoxide rings reacted when 365 nm light was used for initiation; however, this wavelength did not initiate the cationic polymerization when DAI was used alone. Since

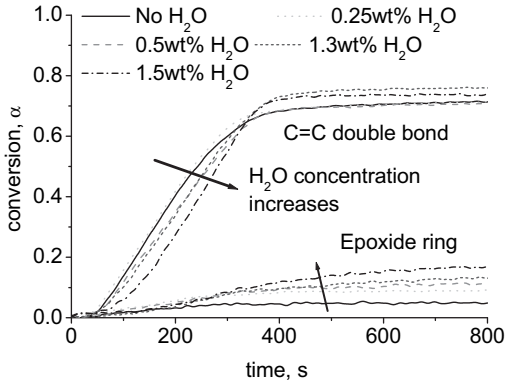

Fig. 6. Conversion profiles (by real-time Raman spectroscopy) of METHB formulated with different water concentrations and photopolymerized with a dual-initiator system (0.5 wt% DMPA and 0.5 wt% DAI). Samples were cured with 100 mW/cm^2 initiation light intensity at room temperature.

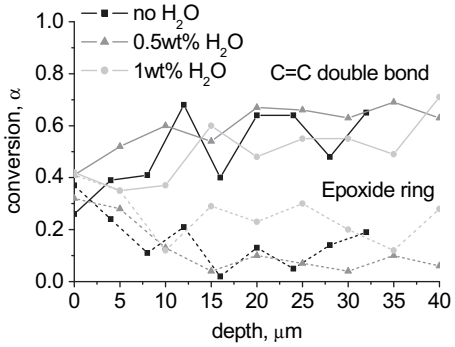

Fig. 7. Depth profiles (by Raman confocal spectroscopy) of METHB formulated with different water concentrations and photopolymerized with a dual-initiator system (0.5 wt% DMPA and 0.5 wt% DAI). Solid lines and dashed lines represent the after-illumination conversion of C═C double bond and epoxide ring, respectively. Samples were cured with 100 mW/cm^2 initiation light intensity at ambient conditions.

DMPA can undergo photodecomposition under illumination of a higher wavelength light than DAI, the effective initiation wavelength of DAI can be extended to the effective illumination window of DMPA when DMPA and DAI are used together.

The effect of water on the epoxide and methacrylate conversions after full illumination is shown as a function of depth in Fig. 7. Although the experimental conditions between the real-time specimens (capillary tubes with 500 s illumination) and the depth-profiling specimens (films with 45 min illumination) are not exactly the same, the bulk conversions for the epoxide and acrylate are comparable in Fig. 6 (after 400 s) and Fig. 7 (below 15–20 μ). In general, the depth profile of the three coatings also matched the real-time study results: higher conversions of both functional groups were realized with increasing water concentration. The conversions of the C═C double bond are lower at the surface from 0–10 μm due to oxygen inhibition [16]. However, with the higher conversion of epoxide ring at the surface, the coatings achieved good surface qualities. Similar to the behavior of the DAI-only system discussed in the previous section, the depth profile of the coating with 0.5 wt% water added was close to the profile of the coating with no water added. When larger amounts of water were added, as shown in the coating with 1 wt% water added, the epoxide ring conversion at the coating interior was much higher than the other two systems due to extensive chain transfer.

After 24 h dark storage (see Fig. 8), the epoxide ring conversion in all coatings, regardless of water added, increased and was

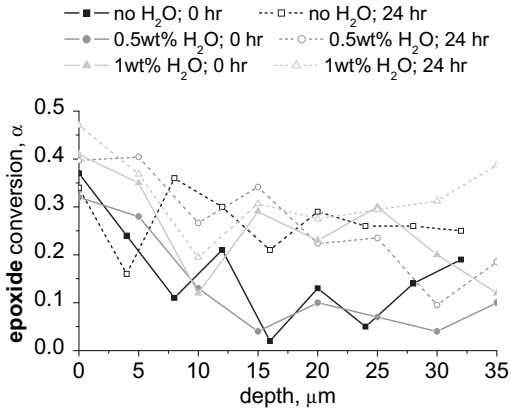

Fig. 8. Depth profiles (by Raman confocal spectroscopy) of epoxide ring conversion in METHB formulated with different water concentrations and photopolymerized with a dual-initiator system (0.5 wt% DMPA and 0.5 wt% DAI). Solid lines and dashed lines represent the conversion of epoxide rings at 0 and 24 h after illumination, respectively.

consistent throughout the coating depth. In contrast to the results of dark polymerization in the DAI-only coatings, similar ultimate conversion of the epoxide ring was measured in the depth profiles after dark storage, even though the epoxide ring conversion was higher with increasing water concentration when measured immediately after 45 min illumination. The high conversions of the acrylate C═C double bond, which were similar regardless the water concentration, defined the polymer matrix formed in these coatings. Thus, mobility of the cationic centers in all coatings was constrained during dark polymerization by the free volume of polymer matrix, resulting in only 20–40% conversion, rather than the 50–60% conversion observed in the DAI-only coatings (Fig. 5).

3.4. Physical property testing

Surface hardness tests and DMA experiments were carried out to determine how increasing water concentration altered physical properties of the coating. All coatings were stored in the dark for 48 h to ensure that no substantial reaction of the epoxide rings occurred while samples were tested under elevated temperatures.

3.4.1. Surface hardness testing of the photopolymer coatings

Pencil hardness tests based on ASTM D33363 were performed on all coatings (see Table 1). The formulations containing only free-radical initiator resulted in tacky surfaces due to oxygen inhibition, and the testing results are not listed in Table 1. However, all formulations containing DAI only and the dual-initiator system showed 6H gouge hardness no matter the concentration of the water. Since the DAI-only system produces a linear polymer, the surface quality depends on the epoxide ring conversion and the polymer chain length. With the addition of 0.5–1.3 wt% water, the scratch hardness stayed at 3H and then decreased to 2H when 1.5 wt% water was added. Thus, for METHB, a low concentration of water did not significantly degrade the surface quality. However, a high concentration of water could deteriorate the surface quality due to shorter polymer chains and lower molecular weight caused by extensive chain transfer. In contrast, water did not show any impact on the surface scratch hardness of coatings cured by the dual-initiator system, which demonstrates the lower sensitivity of the hybrid resin system to the atmospheric factors, such as oxygen and water.

3.4.2. Physical properties evaluated by DMA

The effect of water on the glass transition temperature and storage moduli of METHB coatings cured with the 0.5 wt% DAI-only system and with the dual-initiator system (0.5 wt% DMPA and 0.5 wt% DAI) was determined through temperature ramping studies by dynamic mechanical analysis (DMA). The METHB coatings with different water concentrations photopolymerized with DMPA were omitted because these coatings had oily surfaces and

Table 1
Comparison of surface hardness of the resulting photopolymer coatings.

Initiator system	H_2O concentration (wt%)	Pencil hardness	
		Gouge	Scratch
0.5 wt% DMPA only	All formulations	Tacky surface	
0.5 wt% DAI only	0	6H	3H
	0.5	6H	3H
	1	6H	3H
	1.3	6H	3H
	1.5	6H	2H
0.5 wt% DMPA + 0.5 wt% DAI	0	6H	5H
	0.5	6H	5H
	1	6H	5H
	1.3	6H	5H
	1.5	6H	5H

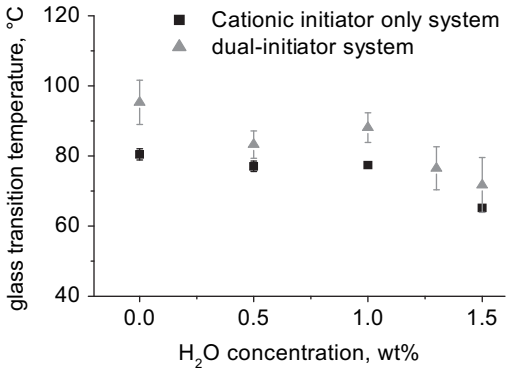

Fig. 9. Glass transition temperature (by DMA), which was determined by the tan δ peak, of METHB coatings formulated with different water concentrations and photopolymerized with 0.5 wt% DAI only and with a dual-initiator system (0.5 wt% DMPA and 0.5 wt% DAI). Coatings were stored in the dark for 48 h before experiments.

water did not show a large impact on the free-radical polymerizations. Fig. 9 shows the T_g of the METHB coatings with different water concentrations photopolymerized with DAI only and with the dual-initiator system. In general, the coatings cured with the dual-initiator system had higher T_g than those cured with DAI only because the dual-initiator system resulted in cross-linked polymers mainly formed through acrylate C═C bonds. Polymers with DAI only were linear, with linkages through the epoxide rings. In both systems, increasing water concentration resulted in decreased T_g. This trend agrees with what has been observed with other polar polymers, such as nylon [40].

For DAI-only systems, the T_g decreased 15 °C when the water concentration increased from 0 to 1.5 wt%. After a decrease of 3 °C occurred with the addition of 0.5 wt% water, the T_g did not change appreciably when the water concentration increased to 1 wt%; however, the T_g dropped 12 °C when the water concentration increased to 1.5 wt%. This phenomenon agrees with the pencil hardness test result, as well as the kinetic and depth-profile studies. Very small amounts of water inhibited the cationic polymerization, decreased the ultimate conversion, and thus decreased the T_g; large amounts of water resulted in decreased T_g and deteriorated surface hardness as explained in the previous section [17,41].

For dual-initiator systems, since the methacrylate C═C double bonds react more quickly than the epoxide rings and a cross-linked network is being formed, the mobility of the cationic reactive centers was further decreased due to vitrification. As water was added to the dual-initiator systems, the consumption of epoxide rings has many different pathways: (1) monomers propagate through the ACE mechanism and form polymer chains with –C–C–O– backbones and C═C pendant groups; (2) monomers or epoxide pendant groups react with another free or pendant unreacted epoxide ring through the ACE mechanism, and some may result in cross-linking; (3) monomers react with water through the AM mechanism and form diols, which can participate in reactions later; (4) epoxide ring pendant groups react with water or diols through the AM mechanism and form –OH pendant groups on the polymer chains; and (5) monomers or epoxide pendant groups react with free or pendant –OH groups, and some may result in cross-linking. The most probable pathways depend on the concentration of the monomer, pendant epoxide rings, water, and free and pendant –OH groups. Instead of decreasing the molecular weight and polymer chain length as in the DAI-only systems, water may also change the cross-linking density and side groups on polymer chains in the dual-initiator systems. In general, the increase of cross-linking density, pendant group size, and intramolecular bonding, such as hydrogen bonding among –OH groups, increases the T_g. However,

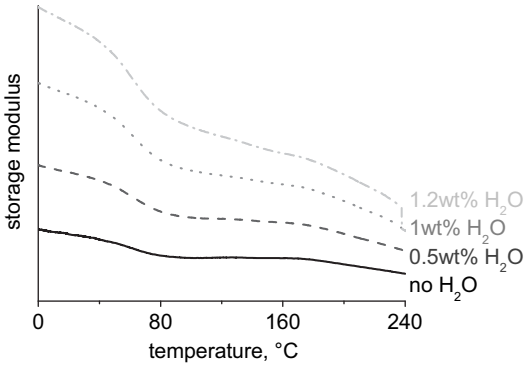

Fig. 10. Stacked storage modulus vs. temperature curves of METHB coatings formulated with different water concentrations and photopolymerized with a dual-initiator system (0.5 wt% DMPA and 0.5 wt% DAI). Coatings were stored in the dark for 48 h before experiments. These DMA profiles are in MPa, but were multiplied by an arbitrary constant to make comparison of the features easier.

due to the complexity of this system, the contribution from each factor is extremely difficult to quantify.

The effect of water on the storage moduli of METHB coatings cured with the dual-initiator system (0.5 wt% DMPA and 0.5 wt% DAI) is shown in Fig. 10. The films showed signs of degradation after removal from the DMA, namely yellowing and aging, which may explain the decrease in modulus observed at high temperatures. The degradation may be a result of disruption of interchain hydrogen bonding in the epoxide network due to the presence of moisture and/or thermal instability related to a ceiling temperature of ~200 °C reported for epoxides [42].

A clear rubbery plateau, rising slightly with temperature, is present for coatings with no water added, which indicates the formation of a cross-linked polymer network. As the water concentration was increased, the slope of the storage modulus-temperature curve above the T_g increased and suggested decreasing cross-linking density. However, the T_g shown in Fig. 9 decreased 8 °C for the coating with 0.5 wt% water, then increased 5 °C for the coating with 1 wt% water, and started to decrease as more water was added. With the information available, a possible explanation is proposed as follows. As 0.5 wt% water was added to system, the deactivation of the photoinitiator resulted in a lower cationic active center concentration, a lower cross-linking density, and a lower T_g. At intermediate water concentrations, more epoxide rings were consumed through the AM mechanism, and a large amount –OH groups were formed. Since most of the epoxide rings were bonded to polymer chains, larger side groups or cross-links were formed after the water was consumed, resulting in an increase of the T_g. However, when excessive amounts of water were added, at similar values of ultimate conversion, most of the epoxide rings may form diols through the AM mechanism and be trapped without further propagation. Thus, the side groups and cross-linking density would be smaller than in systems with lower water concentration, resulting in a lower T_g.

4. Conclusion

Water concentration greatly impacted the epoxide ring-opening polymerization in formulations of the methacrylate/epoxide hybrid monomer METHB with cationic initiator or dual-initiator systems, but had little effect in formulations with only free-radical initiator. With increasing water concentration, the induction period increased as only the cationic initiator was used; however, the induction period disappeared when using the dual-initiator system due to free-radical promoted decomposition of the cationic photoinitiator. The ultimate conversion of epoxide ring depends on the active center concentration and the accessibility of unreacted epoxide rings, which is determined by the free volume of the polymer; thus, the ultimate conversion of coatings with no water added cured by only the cationic initiator was higher than in coatings with water added if given enough time to react further in the dark. The ultimate conversions of coatings cured by the dual-initiator system with different water concentrations were similar because of the constraint placed by the formation of polymer chains through the free-radical polymerization of the methacrylate.

Large amounts of water decreased the surface hardness of coatings cured by only the cationic initiator; whereas, no significant impact was observed in coatings cured with the dual-initiator system. For systems with only the cationic initiator, the T_g generally decreased with increasing water concentration because chain transfer reactions result in shorter polymer chains and lower molecular weight. For dual-initiator systems, cross-linking densities decreased as the water concentration increased. Thus, hybrid systems were shown to be less sensitive to water at low or intermediate concentrations. When the water concentration was too high, hybrid monomer systems manifested decreased physical properties due to loss of cross-linking.

Acknowledgements

This material is based upon work supported by the National Science Foundation under Grant No. 0133133 and the University of Iowa. We would like to acknowledge Daicel and Sartomer for providing the materials used in this study.

References

[1] Fouassier JP. Photoinitiation, photopolymerization, and photocuring: fundamentals and applications. New York: Hanser Publishers; 1995.
[2] Koleske JV. Radiation curing of coatings. West Conshohocken: ASTM International; 2002.
[3] Fouassier JP, Rabek JF. Radiation curing in polymer science and technology. In: Practical aspects and applications, vol. IV. New York: Elsevier Applied Science; 1993.
[4] Crivello JV. Advances in Polymer Science 1984;62:1–48.
[5] Crivello JV, Lam JHW. Journal of Polymer Science Part A Polymer Chemistry 1979;17(4):977–99.
[6] Roffey CG. Photopolymerization of surface coatings. New York: John Wiley & Sons, Inc.; 1982.
[7] Decker C, Nguyen Thi Viet T, Decker D, Weber-Koehl E. Polymer 2001;42(13):5531–41.
[8] Oxman JD, Jacobs DW, Trom MC, Sipani V, Ficek B, Scranton AB. Journal of Polymer Science Part A Polymer Chemistry 2005;43(9):1747–56.
[9] Cho JD, Hong JW. Journal of Applied Polymer Science 2004;93(3):1473–83.
[10] Dean KM, Cook WD. Polymer International 2004;53(9):1305–13.
[11] Cook WD, Chen F, Ooi SK, Moorhoff C, Knott R. Polymer International 2006;55(9):1027–39.
[12] Lin Y, Stansbury JW. Polymer 2003;44(17):4781–9.
[13] Dean K, Cook WD, Zipper MD, Burchill P. Polymer 2001;42(4):1345–59.
[14] Rajaraman SK, Mowers WA, Crivello JV. Journal of Polymer Science Part A Polymer Chemistry 1999;37(21):4007–18.
[15] Rajaraman SK, Mowers WA, Crivello JV. Macromolecules 1999;32(1):36–47.
[16] Cai Y, Jessop JLP. Polymer 2006;47:6560–6.
[17] Crivello JV, Ortiz RA. Journal of Polymer Science Part A Polymer Chemistry 2002;40(14):2298–309.
[18] Hartwig A, Schneider B, Lühring A. Polymer 2002;43(15):4243–50.
[19] Sangermano M, Malucelli G, Morel F, Decker C, Priola A. European Polymer Journal 1999;35(4):639–45.
[20] Lin Y, Stansbury JW. Polymers for Advanced Technologies 2005;16(2-3):195–9.
[21] Sangermano M, Bongiovanni R, Priola A, Pospiech D. Journal of Polymer Science Part A Polymer Chemistry 2005;43(18):4144–50.
[22] Bednarek M, Biedron T, Kahluzynski K, Kubisa P, Pretula J, Penczek S. Macromolecular Symposia 2000;157:1–11.
[23] Kubisa P, Bednarek M, Biedron T, Biela T, Penczek S. Macromolecular Symposia 2000;153:217–26.
[24] Kubisa P. Makromolekulare Chemie-Macromolecular Symposia 1988;13–14:203–10.
[25] Hartwig A, Harder A, Lühring A, Schröder H. European Polymer Journal 2001;37(7):1449–55.
[26] Yagci Y. Macromolecular Symposia 2006;240:93–101.
[27] Lin Y, Stansbury JW. Journal of Polymer Science Part A Polymer Chemistry 2004;42(8):1985–98.

[28] Nelson EW, Scranton AB. Journal of Polymer Science Part A Polymer Chemistry 1996;34(3):403–11.
[29] Gauthier MA, Stangel I, Ellis TH, Zhu XX. Journal of Dental Research 2005;84(8):725–9.
[30] Reinecke H, Spells SJ, Sacristan J, Yarwood J, Mijangos C. Applied Spectroscopy 2001;55(12):1660–4.
[31] Kozanecki M, Zientarska J, Ulanski J. Macromolecular Symposia 2002;184: 299–309.
[32] Baia L, Gigant K, Posset U, Petry R, Schottner G, Kiefer W, et al. Vibrational Spectroscopy 2002;29(1-2):245–9.
[33] Aldrich. Applications: free radical initiators. Available at: www.sigmaaldrich.com/img/assets/3900/Photoinitiators.pdf.
[34] Lin-Vien D, Colthup NB, Fateley WG, Grasselli JG. The handbook of infrared and Raman characteristic frequencies of organic molecules. San Diego: Academic Press; 1991.
[35] Nyquist R. Interpreting infrared, Raman, and nuclear magnetic resonance spectra, vol. 1. San Diego: Academic Press; 2001.
[36] Nyquist R. Interpreting infrared, Raman, and nuclear magnetic resonance spectra, vol. 2. San Diego: Academic Press; 2001.
[37] Bi YB, Neckers DC. Macromolecules 1994;27(14):3683–93.
[38] Yagci Y, Schnabel W. Makromolekulare Chemie-Macromolecular Symposia 1992;60:133–43.
[39] Crivello JV, Ortiz RA. Journal of Polymer Science Part A Polymer Chemistry 2001;39(20):3578–92.
[40] Murayama T. Dynamic mechanical analysis of polymeric material. New York: Elsevier; 1978. p. 201–2.
[41] Hartwig A. International Journal of Adhesion and Adhesives 2002;22(5):409–14.
[42] Kaelble D, Moacanin J, Gupta A. Physical and mechanical properties of cured resins. In: May C, editor. Epoxy resins: chemistry and technology. 2nd ed. New York: Marcel Dekker, Inc.; 1988. p. 603–51.